Quantitative study of cementitious materials by X-ray diffraction/ Rietveld analysis using an external standard

G. Le Saoût[1], T. Füllmann[1], V. Kocaba[1], K.L. Scrivener[1]
[1]*Ecole Polytechnique Fédérale de Lausanne (EPFL), Lausanne, Switzerland*

Abstract

Knowledge of the microstructure of hydrated cement is essential for forecasting their performance. Both cement producers and cement researchers have made extensive use of X-Ray Diffraction (XRD) to identify and quantify the crystalline phases in ground cements. However further studies are needed to understand the chemistry and reactivity of hydrating cements. The quantitative phase analysis of hydrated cement using the Rietveld method has been performed to follow the microstructure of a Portland cement paste up to 28 days. The weight fraction of the XRD undetectable phases such as C-S-H is deduced using both the internal and external standard methods.

1. Introduction

One of the most important techniques for characterizing cementitious materials is X-Ray Diffraction (XRD). The XRD in combination with the Rietveld method is a powerful method for the determination of quantitative phase amounts in anhydrous cementitious materials [1, 2]. More recently, this method has also been employed for the quantitative determination of the principal phases in hydrated cement paste [2-4]. However, the presence of ill crystallized materials in hydrated paste such as C-S-H requires the use of internal or external standard using Rietveld method.

In the internal standard method, by using a defined quantity of crystalline standard material mixed with the sample, it is possible to determine the ratio of crystalline material in the sample to the crystalline standard and thus calculate the content of amorphous material in the sample (see [5] and references therein). In the external standard method [6], to avoid complications that might be caused by mixing an internal standard with the sample (problem of homogenization for example) diffraction data may be measured separately for the sample and the standard under the same conditions.

In this study, XRD experiments are carried out in order to compare the two methods on a model mixture composed of anhydrous cement and an amorphous slag. Then, the two methods are applied to the hydrated paste to follow quantitatively the variation of the different phases present with the hydration time. The hydration degree deduced by XRD is then compared with those calculated by Backscattered electron image analysis (BSE/ IA) as previously described in [3].

2. Experimental details

The chemical compositions of the cement and slag used in this study are given in Table 1.

Phases	cement %wt	slag %wt
SiO_2	20.4	31.3
CaO	61.8	36.8
Al_2O_3	4.7	15.9
Fe_2O_3	2.4	0.3
MgO	1.9	9.7
$Na_2O_{eq.}$	0.9	0.6
SO_3	3.0	2.7

Table 1: Chemical composition of the raw materials

Cement and slag were mixed in different weight ratio (from 10:90 to 90:10) using a Tubular mixer for about eight hours. For the internal standard method, 20%wt rutile relative to the weight of cement-slag mixture was added. Particle size measurement by Malvern Mastersizer laser sizing determined the values of particle size (based on the volume weighted D_{50}) for cement and slag to be 11.5 and 12.5 μm respectively.

The cement paste was mixed with distilled water by hand for 2 min at a water to cement ratio (w/c) of 0.4 and cast into a cylinder 30 mm in diameter and 50 mm in length. After setting, the cylinder mould was topped up with water and the sample kept saturated. At the ages of 1, 2, 3, 7, 14 and 28 days, two slices about 4 mm thick were sawn from the cylinder and immediately washed with isopropanol to dry the surface, the slices were then placed in the diffractometer and an XRD pattern acquired. Then the slice was kept about one week in isopropanol to stop hydration and ground (D_{50} = 22.5 μm). The other slice was impregnated with resin and polished to 0.25 μm for examination by BSE-SEM as described in [3]. Portlandite content was also determined by

Thermogravimetric Analyser (TGA, Mettler Toledo) at a heating rate of 10°C.min^{-1} under Nitrogen.

X-Ray Diffraction (XRD) data were collected using a PANalytical X'Pert Pro MPD diffractometer in a θ-θ configuration employing the CuK_α radiation (λ=1.54 Å). The samples were scanned between 7 and 75° with the X'Celerator detector. The ground powder were manually front -loaded into a circular standard sample holders (diameter 3.5 cm) by lightly pressing with a frosted glass side to minimize the preferred orientation. Same sample holders were used for the slice.

All Rietveld refinements were done using the X'Pert High Score Plus program from PANalytical using the following structures for the dominant phases in the anhydrous sample: monoclinic C_3S [7], C_2S [8], C_4AF [9], cubic C_3A [10], gypsum [11], anhydrite [12], periclase [13] and with two other phases for hydrated cement: CH [14], ettringite [15]. The M3 polymorph of C_3S in the anhydrous cement was supported by an inspection of the X-ray diagram (see [16, 17] and the diffraction pattern of M3 polymorph in one of the characteristic angular window in Fig.1). These data concerning the crystalline structures of the phases contained in the cement were included in the so-called control file. Previous work (see [3] and references inside) has led to the development of control files through extensive comparison with model mixtures of synthetic phases and comparison with other techniques.

In the refinement strategy, profile parameters varied (scale factor, the W coefficient to describe the Full-Width at Half-Maximum (FWHM) of the pseudo-Voigt profile function and the lattice parameters) but the atomic parameters retained their original values. Preferred orientation corrections for C_3S, sulfate phases, CH and ettringite were made according to the March model after Dollase [18]. In order to stabilize the refinement, the shifts of these parameters, except scale factor, were damped taking care that no bounding limit is reached when the refinement is finished. Furthermore, the occupancy of Fe and Al atoms in C_4AF was also refined in anhydrous sample with constraint the sum of occupancies in the respective crystallographic positions constant. The background was refined by a fifth-order polynomial function for the anhydrous cement. However, for the mixture containing slag or hydrated paste, the polynomial function cannot well described the amorphous hump then a background correction after Sonneveld algorithm [19] was applied before the refinement.

3. Results and discussion

3.1. Raw materials

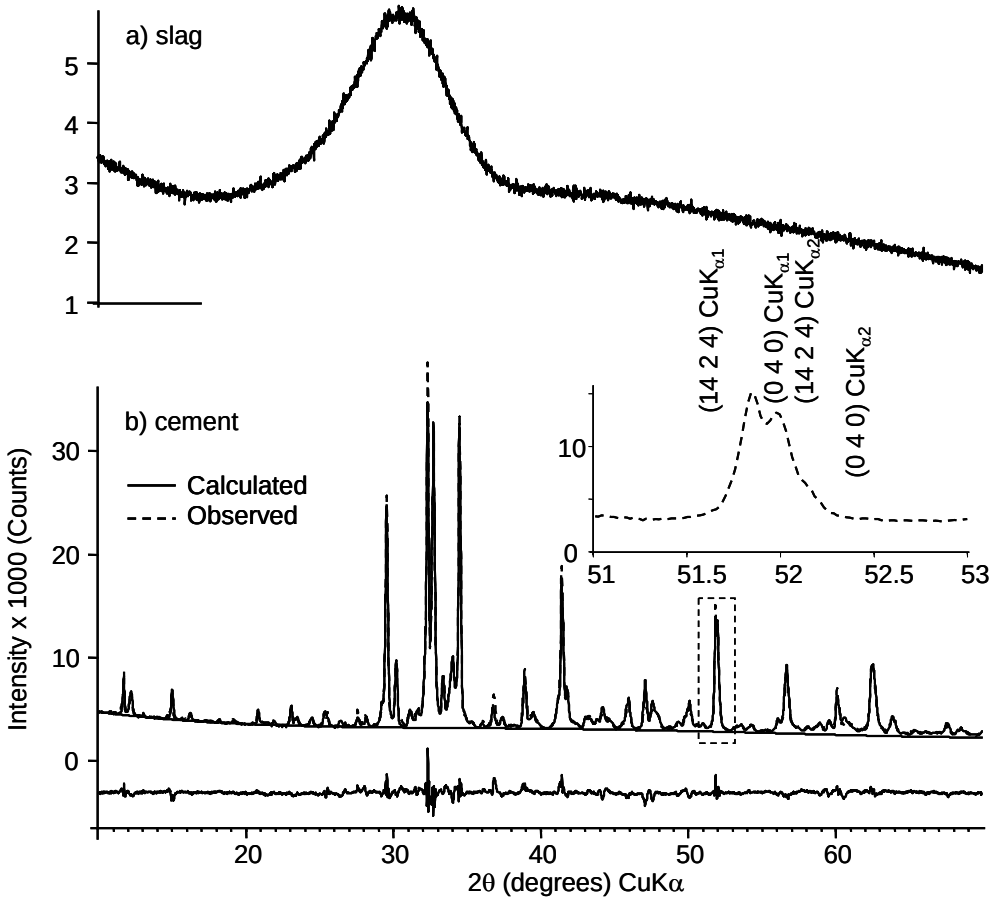

Figure 1 : XRD pattern of the slag (a) observed and calculated patterns for the cement (Rwp = 5.2%, Rexp= 1.5%), the lower curve shows the difference between observed and calculated patterns. One of the angular window (51°-53°) that permits to identify the M3 alite polymorph (b)

The XRD patterns of the raw materials are represented in the Fig.1. The slag contains no crystalline phases (Fig.1.a). The shape and the position of the hump are similar to the main C-S-H pattern. Fig.1.b. shows us the observed and calculated diffraction pattern for the anhydrous cement. The correlation matrix reveals an important correlation between the scale factors of C_2S and C_3S that can be explained by an overlap of the C_2S and C_3S pattern. This can reduce accuracy of estimated phase as previously

noticed [20]. Previous comparison with model mixture leads to an estimation of error of +/- 2% wt on these phases.

3.2. Mixture anhydrous cement-slag

The observed and calculated patterns for a 50:50 cement- slag mixture of are shown in Fig.2.

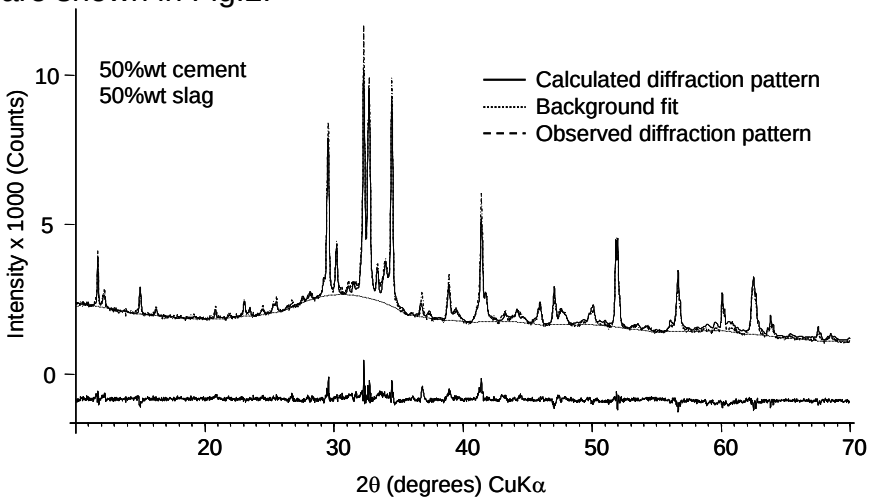

Figure 2 : Observed and calculated diffraction pattern for a 50:50 slag-anhydrous cement mixture (Rwp=5.0%, Rexp=2.2%), the lower curve shows the difference between observed and calculated patterns.

In the internal standard method, the calculation of the slag content in the initial mixture X_{slag} can be calculated using the following equation:

$$X_{slag} = \frac{1}{1 - X_{0,standard}} \left(1 - \frac{X_{0,standard}}{X_{standard}} \right)$$

where $X_{0,\ standard}$ is the added amount of internal standard and $X_{standard}$ the calculated amount of standard by the Rietveld method. However, as pointed out by Taylor *et al.* [2], if we assume an absolute 0.5 per cent error in $X_{standard}$, it is doubtful whether amorphicity levels below 10 per cent could be detected. Furthermore, absolute error is also certainly present in $X_{0,\ standard}$ (as an example, the amorphous content of the NIST SRM676 corundum standard was though to be 2% but has been recently revised to be 8% [4]). The content of amorphous phase in anhydrous cement is also still controversial [21]. So, the relative error increases at low amorphous content because the uncertainly is larger. Down to 10%wt, the correlation of the actual weight and analyzed amount of the slag content by the internal standard method is quite good as shown in Fig. 3.

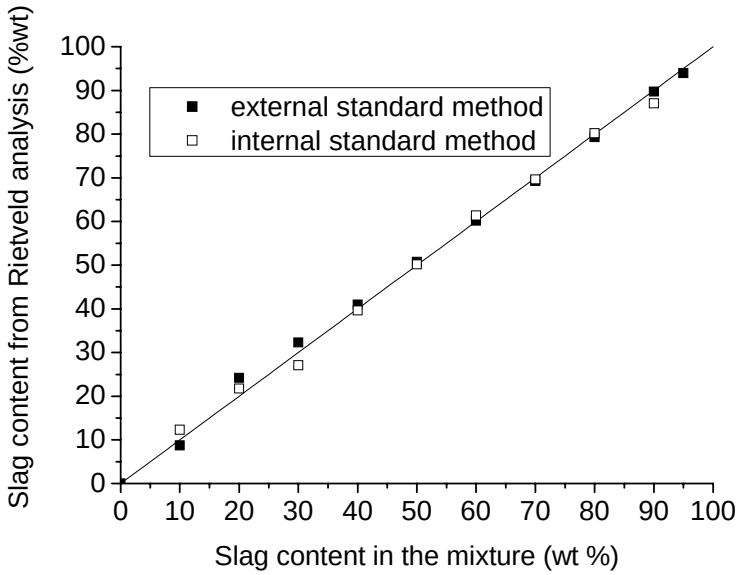

Figure 3 : Comparison between the actual weight and Rietveld analyzed amount of slag in cement – slag model mixtures.

In the external standard method, diffraction data are measured separately for the sample and the standard under the same conditions. The difficulty is to know the relative weight percent of the standard and sample. The model mixture OPC-slag can be used as a calibration and the use of a 51.5:48.5 OPC slag mixture condition leads to the results presented in Fig.3 for the external standard method. There is a good correlation between the two methods with the advantage for the external standard method to have no physical mix to do.

3.3. Hydrated paste

The diffraction pattern for the 28 days hydrated cement is presented in Fig.4. The visual fit reveals the presence of unfitted large peaks at about 29° and 50° (2θ CuK_α) that correspond to the ill crystallized phase C-S-H (PDF file n° 33-0306, $Ca_{1.5}SiO_{3.5}$ xH_2O). The C-S-H pattern can not be included in the control file and refined due to the lack of structural data. The overlap of the large peak at 29° with one the main C_3S peak lead to significant correlations between the W parameter of C_3S and the scale factors of C_3S and C_2S.

We can also observe a large peak at low angle around 10.5° attributed to AF_m phases. As previously noticed by comparing XRD and ^{27}Al NMR

experiments [22], some AF_m phases may be difficult to observe by XRD method indicating the low crystallinity of these phases.

The effect of stopping hydration has also been investigated on the same slice after one week in isopropanol. We can notice a decrease of the ettringite peak and transformation of the AF_m phases. As an example, in system containing calcite, the hemicarbonate diffraction peak disappears when stopping hydration with isopropanol. Except the low angle range concerning AF_t and AF_m phases, diffractograms are much closed and lead to similar results. The same slice has also been ground (D_{50} = 22.5 μm). Although the preparation of materials is quite different, diffractograms are much closed (except low angles) and lead to similar quantitative results. This comparison has also been done at early age (two days) to ensure the validity of the external standard method.

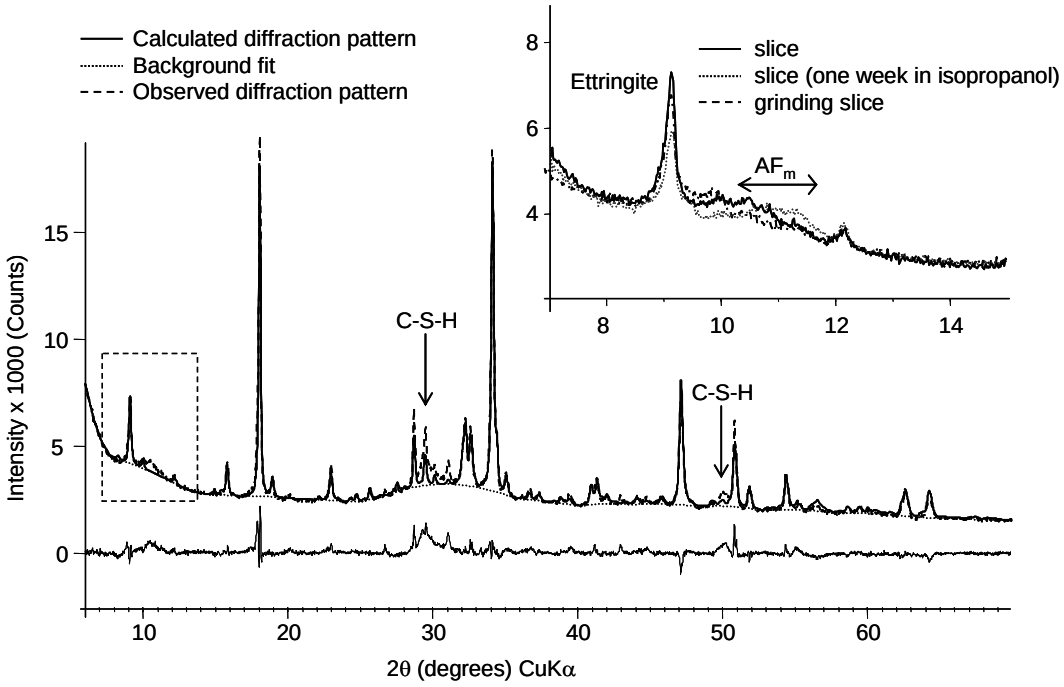

Figure 4: Observed and calculated diffraction pattern for a 28 days hydrated cement (Rwp= 5.9%, Rexp=2.0%), the lower curve shows the difference between observed and calculated patterns. In the upper right corner, influence of isopropanol for the cement hydrated at 28 days.

The output from the Rietveld quantification includes all crystalline and amorphous phases, hydrates and non-hydrates, except water. We should notice that this system cannot be considered as closed, because external mass (water) enters during hydration and some cations from solid phases

are dissolved in the solution. The variation with hydration time of the four main clinker phases content is shown in Fig. 6.a.b. In the first few days the rate of hydration of the anhydrous phases proceeds in the order aluminate, alite, ferrite and belite. The variation with time of the main hydrated products (CH, ettringite and amorphous) are presented in Fig.6.c. The portlandite content was also determined by TGA and we can observed a close agreement between XRD and TGA results although the portlandite content deduced from TGA measurements is systematically lower. The exact amount of Portlandite is difficult to know due to the numerous sources of errors of these two techniques (for TGA: carbonation of CO_2, determination of the weight loss with constructing tangents to the leading and trailing portions of the TG curve depends on the experimentalist).

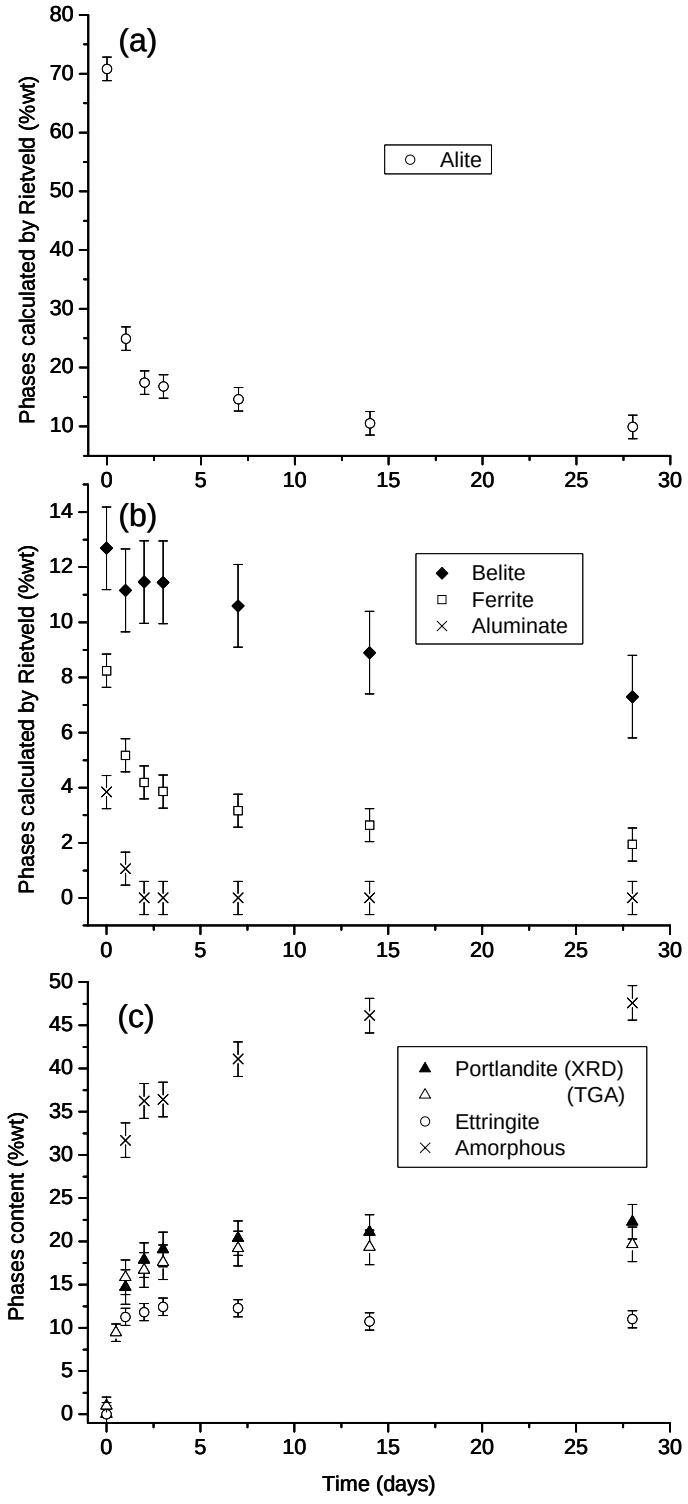

Figure 5: Amounts of the different anhydrous cement phases remaining (a, b) and hydrated products (c).

The degree of hydration was also calculated by simply added the portlandite, ettringite and amorphous content deduced by Rietveld analysis. The comparison of the degree of hydration calculated by BSE/IA (see [3] for further details) and XRD techniques are shown in Fig.7 and shows a good correlation.

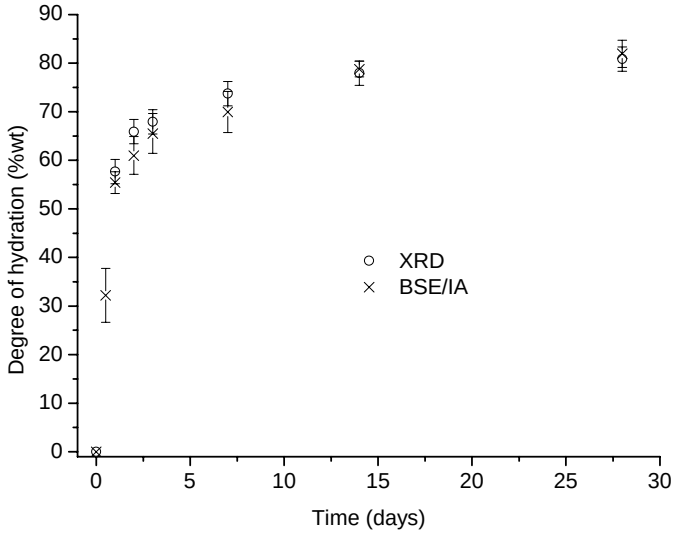

Figure 6: Comparison of the degree of hydration calculated by XRD and BSE/ IA.

4. Conclusion

XRD experiments on a model mixture validate the use of the external standard method to calculate the amorphous content. This method applied to the cement paste has the advantage over the internal standard method to avoid stopping hydration, grinding and mixing the standard with the sample. However a precise calibration of the external standard has to be performed with model mixture. This method has been applied to cement paste and the amount of phases deduced from Rietveld analysis shows good general agreement with other results from TGA and BSE/IA techniques.

However, further research is needed to improve the quality of the fit and determine the influence of refinement parameters. The incorporation of improved existing structure models such as the recent ettringite structure [23] or structure models to determine (such as hemicarbonate) have to be included in the control file. Indeed, a comparison of the different amount of

cement phases deduced by Rietveld analysis with the thermodynamic modeling predictions [24] will be fruitful.

Acknowledgements

V. Kocaba would like to acknowledge the financial support of NANOCEM.

References

[1] G. Walenta, T. Füllmann, Advances in quantitative XRD analysis for clinker, cements, and cementitious additions, Powder Diffr. 19 (2004) 40-44.
[2] J.C.Taylor, L.P. Aldridge, C.E. Matulis, I. Hinczak, X-ray powder diffraction analysis of cements, in J. Bensted, P. Barnes (Eds.), Structure and Performance of Cements, Taylor & Francis, 2001, pp. 420-441.
[3] K.L. Scrivener, T. Füllmann, E. Gallucci, G. Walenta, E. Bermejo, Quantitative study of Portland cement hydration by X-ray diffraction/ Rietveld analysis and independent methods, Cem. Concr. Res. 34 (2004) 1541-1547.
[4] L.D. Mitchell, J.C. Margeson, P.S. Whitfield, Quantitative Rietveld analysis of hydrated cementitious systems, Powder Diffr. 21 (2006) 111-113.
[5] R. Jenkins, R.L. Snyder, Introduction to X-ray Powder Diffractometry, in Chemical Analysis a series of monographs on chemistry and its applications, J.D. Winefordner (Ed.), Wiley, 1996, pp. 138.
[6] P.M. Suherman, A. van Riessen, B. O'Connor, D. Li, D. Bolton, H. Fairhust, Determination of amorphous phase levels in Portland cement clinker, Powder Diffr. 17 (3) (2002) 178-185.
[7] F. Nishi, Y. Takeuchi, I. Maki, Tricalcium silicate Ca_3O (SiO_4): The monoclinic superstructure, Z. Kristallogr. 172 (1985) 297-314.
[8] T. Tsurumi, Y. Hirano, H. Kato, T. Kamiya, M. Daimon, Crystal structure and hydration of belite, Ceram. Trans. 40 (1994) 19-25.
[9] A.A. Colville, S. Geller, The Crystal Structure of Brownmillerite, Ca_2Fe AlO_5, Acta Cryst. B, 27 (1971) 2311-2315.
[10] P. Mondal, J.W. Jeffery, The crystal structure of tricalcium aluminate, $Ca_3Al_2O_6$, Acta Cryst. B, 31 (1975) 689-697.
[11] W.F. Cole, C.J. Lancucki, A refinement of the crystal structure of gypsum $CaSO_4(H_2O)_2$, Acta Cryst. B, 30 (1974) 921-929.
[12] F.C. Hawthorne, R.B. Ferguson, Anhydrous Sulfates II. Refinement of the Crystal Structure of Anhydrite, Canadian Mineral. 13 (1975) 289-292.
[13] D. Taylor, Thermal expansion data. I. Binary oxides with the sodium chloride and wurtzite structure MO, J. British Ceram. Soc. 83 (1984) 5-9.
[14] H.E. Petch, The hydrogen positions in portlandite, $Ca(OH)_2$, as indicated by the electron distribution, Acta Cryst. B, 14 (1961) 950-957.

[15] A.E. Moore, H.F.W. Taylor, Crystal structure of Ettringite, Acta Cryst. B, 26 (1970) 386-393.
[16] M. Courtial, M.-N. de Noirfontaine, F. Dunstetter, G. Gasecki, M. Signes-Frehel, Polymorphism of tricalcium silicate in Portland cement: A fast visual identification of structure and superstructure, Powder Diffr. 18 (2003) 7-15.
[17] M.-N. de Noirfontaine, F. Dunstetter, M. Courtial, G. Gasecki, M. Signes-Frehel, Polymorphism of tricalcium silicate, the major compound of Portland cement clinker. 2. Modelling alite for Rietveld analysis, an industrial challenge, Cem. Concr. Res., 36 (2006) 54-64.
[18] W.A. Dollase, Correction of intensities for preferred orientation in powder diffractometry: Application of the March model, J. Appl. Cryst. 19 (1986) 267-272.
[19] E.J. Sonneveld, J.W. Visser, Automatic collection of powder data from photographs, J. Appl. Cryst. 8 (1975) 1-7.
[20] O. Pritula, L. Smrcok, B. Baumgartner, On reproducibility of Rietveld analysis of reference Portland cement clinkers, Powder Diffr., 18 (2003) 16-22.
[21] P.S. Whitfield, L.D. Mitchell, Quantitative Rietveld analysis of the amorphous content in cements and clinkers, J. Mat. Sci. 38 (2003) 4415-4421.
[22] G. Le Saoût, E. Lécolier, A. Rivereau, H. Zanni, .Chemical structure of cement aged at normal and elevated temperatures and pressures, Part I: Class G oilwell cement, Cem. Concr. Res., 36 (2006) 71-78.
[23] F. Goetz- Neunhoeffer, J. Neubauer, Refined ettringite ($Ca_6Al_2(SO_4)_3(OH)_{12}\ 26H_2O$) structure for quantitative X-ray diffraction analysis, Powder Diffr. 21 (2006) 4-11.
[24] B. Lothenbach, F. Winnefeld, Thermodynamic modeling of the hydration of Portland cement, Cem. Concr. Res., 36 (2006) 209-226.